Cloud removal on satellite imagery using blended model: case study using quick look of high-resolution image of Indonesia

Muhammad Dimyati[1], Adlyani Husna[2], Puji Tri Handayani[2], Devy Nur Annisa[2]
[1]Department of Geography, Faculty of Mathematics and Natural Sciences, Universitas Indonesia, Depok, Indonesia
[2] PT. Terramitra Citra Persada, Grand Center Blok H No. 41, Kebayoran Baru, Jakarta 12160, Indonesia

Article Info

Article history:

Received Jul 14, 2021
Revised Feb 17, 2022
Accepted Feb 25, 2022

Keywords:

Blended cloud removal model
High-resolution image
Quick look image
Satellite image

ABSTRACT

The problem with the acquisition of satellite imagery in the tropics, especially in the area around the equator is that it is almost covered by clouds throughout the year. Users need cloud cover information and the possibility of obtaining cloudless satellite images before they get the data. An overview of the availability of cloud coverage distribution, especially those presented in a spatial format, was very beneficial and increased efficiency for users to select image data in the area of interest (AoI). This study aimed to develop a cloud removal, so-called blended cloud removal (BCR) model, which was applied in a part of West Java Province. The data used for this study were 33 images of quick looks at high-resolution satellite images of the 2013-2015 period that could be obtained free of charge on the website. The results showed that the distribution of efficiency was that AoI-1 obtained 99.67% efficiency of cloud removal image, AoI-2 was 76.51%, and AoI-3 obtained 98.34%. These three AoI locations have an average efficiency of 91.50%. As a result, there was substantial evidence that fewer than 10% of cloud cover remains after cloud removal. This suggests that by using the BCR model, a considerable change in cloud cover for the AoI location might be obtained, meeting the Geospatial Information Agency's standards.

Corresponding Author:

Muhammad Dimyati
Department of Geography, Faculty of Mathematics and Natural Sciences, Universitas Indonesia
Jalan Margonda Raya, Pondok Cina, Depok, 16424, Indonesia
Email: m.dimyati@sci.ui.ac.id

1. INTRODUCTION

Basic spatial information on a large scale is one of the most needed variables in supporting regional development. The requirement for large-scale mapping for the entire territory of Indonesia to support regional development is highly urgent and essential. Therefore, accelerating the provision of large-scale geospatial data is very important for better spatial planning and regional development. The main challenges to resolving large-scale geospatial data are limited resources, particularly financial resources, and a lack of time for terrestrial measurements in the field. The presence of satellite imagery, however, can help to solve these problems. Measurements using satellite imagery can accelerate the completion of essential geospatial data generation. In addition, the use of satellite imagery is also cheaper than field measurements for an extensive area. However, the main problem that is often encountered in satellite image procurement is cloud cover [1]. In many locations in Indonesia, particularly around the equatorial areas, the availability of cloud-free optical satellite imagery is relatively low. The availability of cloud-free optical satellite images for a location in the area is rather challenging because the most of the available optical satellite images are cloud-covered.

Even though the need for remote sensing satellite data for areas around the equator is quite high because the developments in that area are also quite developed.

One reason is that the area around the equator is almost covered by clouds throughout the year. Equatorial regions receive more solar irradiance than other parts of the world, causing a band of low pressure to form across the equatorial regions known as the intertropical convergence zone (ITCZ). The oceans cover a large portion of the equatorial area, and solar irradiance causes massive amounts of evapotranspiration over these oceans. However, the humidity level in the equatorial air is high because warm weather has a higher humidity capacity. When air currents from surrounding high-pressure regions blow toward the ITCZ, they bring vast amounts of humidity into the ITCZ, and this wet air rises into the ITCZ and forms cumulonimbus clouds [2]. Satellite images that meet the specified requirements are large-scale images with a cloud cover of 10% per scene. In terms of limited satellite image data, the cloud cover maybe 10% of the area of interest (AoI). But cloud cover must not cover essential objects such as social facilities, public facilities, government offices, industrial areas [3].

The requirement for the use of satellite imagery to support regional development is getting higher [4]. This is in line with the more accessible and more affordable access to obtain remote sensing satellite data. Several models for minimizing cloud coverage in satellite images to meet the requirements for data quality or image map requirements have been developed [4]. The pixel-based model has been developed by the University of Maryland team in collaboration with the Australian National Carbon Accounting System (NCAS) team and the Indonesia National Carbon Accounting System (INCAS) team [5], [6]. The tile-based model has been developed by R. D. Dimyati *et al.* with the Indonesia Aeronautics and Space Agency (LAPAN) and Gadjah Mada University team. The model was created to meet the requirements of medium-scale digital data analysis as well as advanced digital classification [4].

Many experts [7]-[15] have developed cloud removal models for large-scale satellite imagery. Li *et al*. [16] investigated a thick cloud removal method based on the stepwise radiometric adjustment and residual correction (SRARC). The SRARC is aimed at effectively removing the clouds in high-resolution images for the generation of high-quality and spatially contiguous urban geographical maps. These models, on the other hand, are for pre-processing purposes in subsequent digital analysis. To aid the efficacy and efficiency of subsequent processes, early information is required, specifically before the researcher acquires satellite data that will be used in future processing to determine the potential of cloud coverage. Techniques for presenting information more quickly at the start are not generally used.

Cloud cover information for each scene is needed, especially for compliance with existing regulatory requirements and also for determining the final quality of the image map to be processed. This means that users can not rely on various digitally developed cloud removal models [17], which are only processed after the satellite image order is obtained by the user. Users need cloud cover information in each scene and certainty of compliance with regulatory requirements [3] cloud cover in each scene before the data is ordered for analysis. Digital processing indeed provides higher accuracy in cloud removal, but the process is intended for purposes once the satellite image data has been obtained by the user. Meanwhile, the speed and certainty of information regarding cloud cover requirements are essential for users before the digital analysis process [18]-[20].

Recently, the government has been encouraging the acceleration of the completion of large-scale base maps through the participation of stakeholders in the geospatial data industry with the same references and standards. Efforts to accelerate the provision of large-scale basic geospatial information need to be carried out in earnest because it has been more than 50 years since the existence of this data has not yet filled half of the territory of Indonesia. However, the need for its use is increasing and is eagerly awaited. To regulate this, the Geospatial Information Agency issued the regulation of the head of the geospatial information agency No. 1 of 2020. The regulation governs the standards for collecting basic geospatial data for the manufacture of large-scale base maps using drones and non-metric cameras. The availability of a base map is essential because it is used as a reference in making thematic maps.

This study develops a model of cloud removal for satellite images. A cloud removal based on the approach of multi-temporal satellite images is proposed. The basic idea of this approach is to detect cloud and cloud shadows by using the difference in reflectance values between clear pixels and cloud and cloud shadow contaminated pixels. A cloud removal model is a blended approach in which the process of removing clouds and their shadows from satellite imagery is software-based and involves numerous steps. At a location covered by clouds and shadows, it will later be patched with zero cloud imagery from a multi-temporal image. The model of cloud removal for satellite images will be used by the user in planning and selecting the scene to be ordered. The model is also able to describe the condition of the cloud-covered area in the period required by satellite imagery users. This study aims to develop a cloud removal model using blended techniques with software, in the case of using a quick look at high-resolution satellite images, which can be obtained free of charge on the website for a part of West Java [21].

2. RESEARCH METHOD

2.1. Materials

The data for the development of the cloud removal model was used from Worldview-2 and Worldview-3 of the high-resolution satellite (HRS) quick look image, with 20 meters of resolution Table 1 and Table 2. The study area was a part of Bekasi, Karawang, Purwakarta, and Bogor (AoI-1), the northern part of Cianjur, the eastern part of Sukabumi (AoI-2), and the Southern part of Cianjur (AoI-3) regions in the West Java Province. The data for the study area was obtained from Maxar Technology [22], in the period of 2013-2015. The data covers three AoI. The area of AoI-1 was 2387.7 km^2, AoI-2 was 911.01 km^2, and AoI-3 was 869.01 km^2. The scene selection of each AoI depends on the availability of scene data in the area. The availability of scene data for the AoI-1 was 15 images, the AoI-2 was ten images, and the AoI-3 was eight images. The coverage location of the study area is shown in Figure 1.

The software used in this research is the Global Mapper, Adobe Photoshop, and ArcGIS. The Global Mapper was used to re-convert image data of the "tiff" format to image data of the "tiff" format, but it has separate "tfw" data from the image of "tiff" that was used. The "tfw" format file is a file that contains the location, scale, and map rotation of the "tiff" image. The "tfw" file needs to be separated from the "tiff" because the image data of the "tiff" format will be edited by a raster using Adobe Photoshop. Adobe Photoshop is a raster editing software that's not related to spatial functions. Adobe Photoshop was used to remove clouds by deleting raster data at cloud locations continuously until there was no coverage at that location or null.

Table 1. Datasheet Worldview-2 satellite [23]

Launch date 13 August 2014	
Orbit altitude	617 km
Orbit type	Sun-synchronous (10:30 am-descending orbit)
Inclination orbit	98°
Orbital period	97 min
Swath (nadir)	13.4 km
Acquisition mode	Synchronous
Re-visitation period	1.1 days (GSD 0.59 m)
Re-visitation period (nadir)	14 days

Table 2. Datasheet Worldview-3 satellite [24]

Launch date 13 August 2014	
Orbit altitude	617 km
Orbit type	Sun-synchronous (10:30 am-descending orbit)
Inclination orbit	98°
Orbital period	97 min
Swath (nadir)	13.4 km
Acquisition mode	Synchronous
Re-visitation period	1.1 days (GSD 0.59 m)
Re-visitation period (nadir)	14 days

The process of mosaicking scenes was carried out using the Global Mapper software after the entire scene of the satellite image had been edited. The result of the editing by the Global Mapper was more mosaic image data with less cloud coverage. The final step of the process was used by ArcGIS software. This process was carried out to analyze the percentage of the area of remaining cloud cover in each mosaic in the AoI.

2.2. Method

The cloud removal method was a method for removing clouds and cloud shadows in optical satellite images. This method is a method that eliminates the appearance of clouds by displaying image data from different times (multi-temporal). The principle used in the cloud removal process was overlapping and superimposing cloudy image data with clean image data, then localizing the cloud area and patching it with a clean image with the help of an algorithm formulation applied to satellite imagery. The proposed technique is called the blended cloud removal (BCR) model. The BCR model was a cloud masking process to replace the cloud cover of a satellite image in a particular scene with the original data of other scenes that are not covered by clouds at the same location. This BCR model was based on the approach of multi-temporal satellite images in the coverage of AoI, where cloud cover and shadows in satellite imagery were removed using software in many steps.

The essential points that must be considered in the cloud removal process to obtain optimal results are [16]:

1) The difference in image data acquisition time between cloudy and cloudless cover image data was not too long;
2) The closer the period of the cloud-covered image with the fill image, the better the results; and
3) The geometry of both image data must be the same and the appearance uniform.

The difference in recording time in the images to be combined was significant because objects on the earth's surface change very quickly. For example, the development of settlements makes land cover data change very quickly. If the merged images do not come from adjacent recordings, the pixel values will be much different. The geometry of the two images data must be the same so that when combined, particular objects at a location will join the object itself in the complementary image. This cloud removal process could be carried out after previously carrying out the map-to-map rectification or ortho-rectification process.

This process, based on one of the satellite image data that has been geometrically corrected, was used as a reference for the other satellite image data. It is intended that the object in the primary satellite image data does not shift when compared to the replacement satellite image data. The diagram showing the steps of the BCR model is shown in Figure 2.

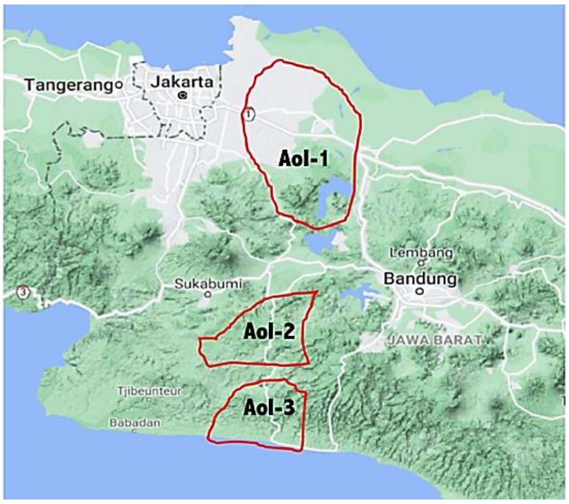

Figure 1. Location of the study area (AoI-1, AoI-2, and AoI-3)

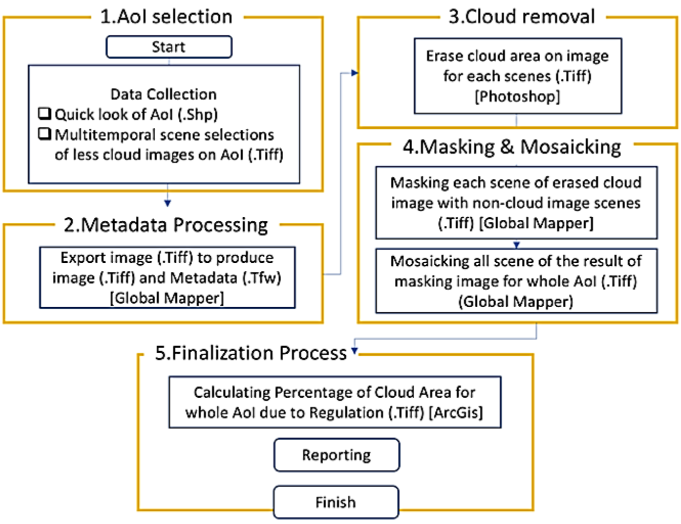

Figure 2. Algorithm of BCR model

The algorithm of the BCR model was carried out as follows:

1) Site selection: site selection of AoI, and identifying cloud-covered scenes in the quick look image, then selection of multi-temporal satellite images for the same location but different acquisition, which could be used to patch the cloud-covered location;
2) Metadata processing: metadata processing is proceeded by exporting image data to the "tiff" format to get a separate image file in the "tiff" and "tfw" format, using Global Mapper software [25];
3) Cloud removal: the cloud removal is done by manually erasing cloud coverage for each scene on AoI, using Adobe Photoshop software [26];
4) Masking and mosaicking: this process is executed by masking with a non-cloud image of the same area from a multi-temporal image. The process is then continued by mosaicking all cloud-free images in the AoI location, and

5) Finalization process: this process includes conducting a spatial analysis of the mosaic of cloud removal image results to calculate the remaining percentage of cloud area to comply with existing regulations (using ArcGis software) [27].

The above algorithm, when formulated in mathematical form, becomes:

$$IBCR = (IOR - ICC) + (IMNC) \quad (1)$$

where: I_{BCR} is the image resulting from blended cloud removal; I_{OR} is the original image that still has cloud cover; I_{CC} is a semi-manually erased cloud cover and its shadow; and I_{MNC} is a multi-temporal image that will be used to patch the I_{CC}. By the regulations of the Geospatial Information Agency, the I_{BCR} must meet the standard requirements of less than or equal to 10%.

3. RESULTS AND DISCUSSIONS

Based on the above algorithm, the cloud removal implementation process was carried out. The BCR model begins with the selection of the AoI location. The chosen image was the result of the acquisition between 2013 and 2015. The 33 scenes chosen show many cloud-covered images before the cloud removal process. To show the coverage of the study area, the 33 scenes were mosaicked, according to their AoI Figure 3.

Figure 3(a) shows a mosaic of AoI-1, covering 15 satellite image scenes. From Figure 3(a), it could be seen that the distribution of cloud cover and its shadows were distributed in small clusters spread evenly throughout AoI. Figure 3(b) shows a mosaic of AoI-2, covering ten satellite image scenes. From Figure 3(b), it could be seen that the distribution of cloud cover and shadows was spreading across the AoI. And Figure 3(c) shows a mosaic of AoI-3, covering eight satellite image scenes. According to Figure 3(c), the distribution of cloud cover and shadows covered several areas and was clustered in specific areas at the AoI location.

The quick look [28] of high-resolution satellite images was georeferenced. But because the cloud removal process would be carried out using editing software raster (Adobe Photoshop), where the software was not software that provides spatial related locations, it was necessary to do the "tiff" conversion. Then the georeferenced "tiff" and "tfw" format files were obtained. The "tfw" format file was a metadata file, which was a file that contained the location, scale, and map rotation of the image ("tiff" format). Because the location files were obtained separately, there would be no issues when editing in Adobe Photoshop. The contents of the information in the "tfw" format file can be seen in Figure 4.

After converting the image and obtaining the "tfw" format file, the image can proceed with the cloud removal steps. Cloud removal was carried out manually using Adobe Photoshop software. Figure 5 shows a part of AoI-1 where the cloud cover has not been removed. After cloud removal, all scene images whose clouds had been removed were displayed and mosaicked using the Global Mapper software. The lowest cloud cover image scene that was at the same acquisition location for a different image scene or multi-temporal scene, was then superimposed, to obtain a cloud-free image scene or an image with low cloud cover as the result of mosaicking the scene image.

Figure 6 shows the results of the final stage of the cloud removal process, which was called the image patching stage in a cloud-covered location with the original coverage on an image with lower cloud cover or cloud-free. Figure 6 shows the results of a part of AoI-1, where the cloud has been removed. The cloud removal procedure was applied to all of the image scenes in the AoI. In this Figure 6, the locations originally indicated by locations 5-A, 5-B, and 5-C have been patched with the other images shown in other temporal images. The new image indicated by location 6-A, location 6-B, and location 6-C shows zero cloud cover.

The enlargement of a part of the area in Figure 5 at location 5-C was shown in Figure 7(a), the area before the cloud removal process. Meanwhile, the enlargement of a part of the area in Figure 6 at location 6-C was shown in Figure 7(b), the area after the cloud removal process. From Figure 5, it was clear that the satellite image was still covered by clouds. After being processed using the BCR model, the results were visible in the area that was originally cloud-covered. It became clear or cloud-free in Figure 6. This clearly shows the effectiveness and success of the BCR model in cloud removal.

After the process of removing clouds and their shadows, then masking and cut-lining with other cloud-free scenes was carried out. The following step was to mosaic them with nearby scenes for the entire AoI. The results of the mosaic after cloud removal can be seen in Figure 8(a), Figure 8(b), and Figure 8(c). To determine whether the cloud cover has met the requirements of less than 10%, as a percentage of meeting the Geospatial Information Agency's regulatory requirements [3], the percentage of cloud cover area has been calculated. Supervised classification was carried out to calculate the percentage of cloud cover area in the final mosaic image result. The supervised classification was carried out through a vectorization process and calculated geometry using ArcGis [26]. The classification was carried out in the whole area of the AoI. The following Table 3 was the result of the percentage of the cloud coverage area for each AoI.

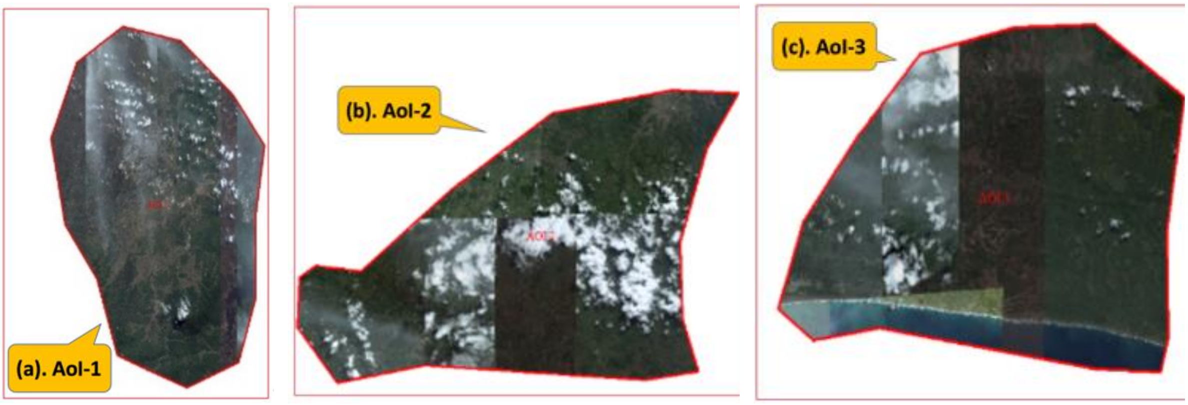

(a) (b) (c)

Figure 3. The area of mosaic from quick look of high-resolution satellite images before cloud removal process: (a) AoI-1, (b) AoI-2, and (c) AoI-3

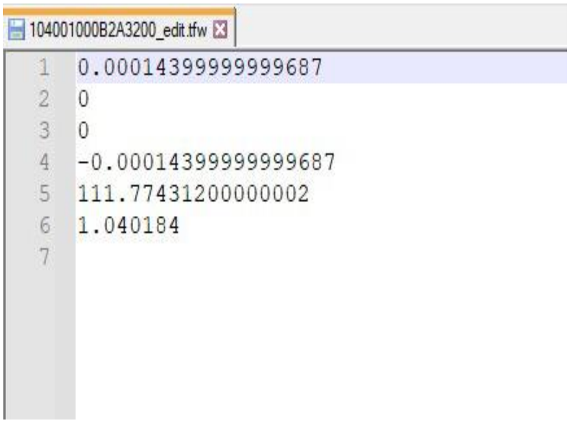

Figure 4. Image of metadata export result

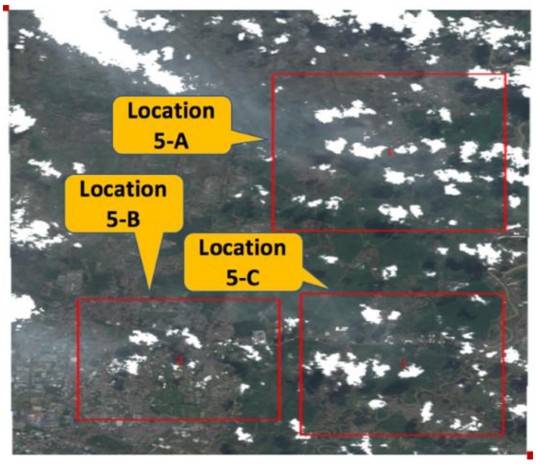

Figure 5. Satellite images as a part of AoI-1 before cloud removal. Location 5-A was covered by dense cloud, location 5-C was covered by medium cloud, and location 5-B was covered by rare clouds

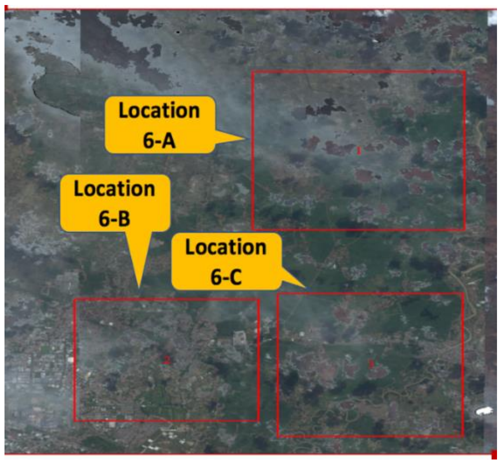

Figure 6. Satellite images as a part of AoI-1 after cloud removal. Location 6-A was zero cloud coverage, location 6-C was zero cloud coverage, and location 6-B was zero cloud coverage

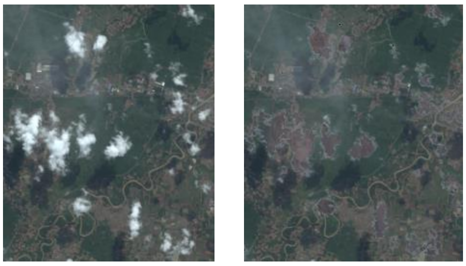

(a) (b)

Figure 7. An enlargement of the image: (a) location 5-C before the cloud removal process and (b) location 6-C after the cloud removal process.

(a) (b) (c)

Figure 8. The area of mosaic from quick look of high-resolution satellite images after the cloud removal process: (a) AoI-1, (b) AoI-2, and (c) AoI-3

Table 3. Area and percentage of cloud cover in AoI

AoI	Area AoI (Km2)	Before cloud removal	After cloud removal
AoI-1	2387.7 km^2	196.695 km^2 (8.2%)	0.657 km^2 (0.02 %)
AoI-2	911.01 km^2	203.933 km^2 (22.4%)	47.912 km^2 (5.2%)
AoI-3	869.01 km^2	65.935 km^2 (7.6 %)	1.096 km^2 (0.13%)

From the analysis results in Table 3, it could be seen that the original AoI-1 was covered by clouds of 196,695 km^2 (8.2%). The cloud cover decreased to 0.657 km^2 (0.02%) after the cloud removal process was completed using the BCR model. The original AoI-2 was covered by clouds of 203.933 km^2 (22.4%). The cloud cover became 47.912 km^2 (5.2%) after the cloud removal process was completed using the BCR model. The cloud coverage was still quite broad because for several years, there were no cloud-free images in the AoI-2 region. The original AoI-3 was covered by clouds of 65.935 km^2 (7.6%). The cloud cover was 1.096 km^2 (0.13%) after the cloud removal process was completed using the BCR model. It could be concluded that AoI-1 obtained 99.67% efficiency of cloud removal image, AoI-2 was 76.51%, and AoI-3 obtained 98.34%. These three AoI's have an average efficiency of 91.50%. Based on this analysis, it was discovered that all of the BCR models resulted in a cloud cover image that was less than or equal to 10% of the Geospatial Information Agency's standard requirements. It could be underlined that there was a significant change in cloud cover for the AoI location before and after cloud removal. These results could explain how the BCR model could be used to assist users in ordering satellite image scenes on AoI with cloud cover close to the planned and by the specified cloud cover requirements. These results would further improve the efficiency of the analysis process on the image scene that would be used for the next stage. Information on the distribution of cloud cover and cloud removal efforts like this will be beneficial for users to choose a location and adjust their budget to procure satellite images to be used.

Research such as cloud removal has been carried out by Li *et al.* [16], which was called stepwise radiometric adjustment and residual correction (SRARC). The concept of SRARC is that the complementary information in adjacent temporal satellite images can be utilized for the seamless recovery of cloud-contaminated areas in the target image after precise radiometric adjustment. To this end, the SRARC method first optimizes the given cloud mask of the target image based on superpixel segmentation, which is conducted to ensure that the labeled cloud boundaries go through homogeneous areas of the target image, to ensure a seamless reconstruction.

The difference between these two studies was that the research conducted by the researchers, called the BCR model, was mainly dedicated to the purpose of digital processing before the data was obtained by the users. Meanwhile, the conducted research [16] was mainly conducted for digital processing after the satellite image data was obtained by the users. The difference between the two studies is very clear. Research conducted by researchers is not carried out by other researchers.

Xu *et al.* [7] conducted research on cloud removal based on sparse representation via a new approach, which was called multi-temporal dictionary learning (MDL). Dictionaries of the cloudy areas (target data) and the cloud-free areas (reference data) were learned separately in the spectral domain. The removal process was conducted by combining coefficients from the reference image, and the dictionary learned from the target image. This method could well recover data contaminated by thin and thick clouds or cloud shadows. Their experimental results show that the MDL method was effective in removing clouds from both quantitative and qualitative viewpoints. Candra *et al.* [8] researched cloud and cloud shadow masking using a multi-temporal cloud masking algorithm in tropical environments. A cloud masking approach based on multi-temporal satellite images was proposed. The basic idea of this approach was to detect cloud and cloud shadows by using the difference in reflectance values between clear pixels and cloud and cloud shadow contaminated pixels. Several bands of satellite images that have a big difference in values were selected for developing the multi-temporal cloud masking (MCM) algorithm. The results show that the MCM algorithm could detect clouds and cloud shadows appropriately. Moreover, qualitative and quantitative assessments were conducted using visual inspections and a confusion matrix, respectively, to evaluate the reliability of this algorithm. Comparisons between this algorithm and the quality assurance (QA) band were conducted to prove the reliability of the approach. The results show that MCM was better than the QA band and the accuracy of the results was very high.

The three researchers mentioned above, Li *et al*. [16], Xu *et al*. [7], and Candra *et al.* [8], conducted cloud removal research for digital analysis of the process after the user owned the satellite image. In addition, the three of them did not use high-resolution image satellites and also did not use quick-look images. Three of them did not calculate the percentage of cloud cover in the study area. This was what distinguishes our research from the research that has been done by many previous researchers.

By the provisions of geospatial information agency regulation No.1 of 2020, which requires that the cloud cover on satellites used in processing basic geospatial information be less than or equal to 10%, BCR could be used as a model to meet the requirements [3], [29]. This means that the BCR model could help accelerate the achievement and efficiency of the regulatory compliance and implementation process. This was consistent with previous research [4], which found that cloud removal could improve the accuracy of selecting input data for the analysis process. These results prove the efficiency and effectiveness of the BCR model in identifying and removing cloud cover from satellite images. Meanwhile, these findings provide a new idea for the remote sensing community, especially in the fields of cloud removal detection and image processing [30].

4. CONCLUSION

In ordering satellite imagery, cloud cover information was essential. In addition to reflecting transparency in the process of providing satellite data acquisition, it will also assist users in increasing the efficiency of data acquisition images in AoI selection. The developed BCR model, which was applied in a part of the West Java Province, using quick look imagery from high-resolution satellite images that could be obtained free of charge on the website, has produced strong scientific evidence. This significant result was shown by a substantial change in cloud cover for the AoI location before and after cloud removal.

The distribution of efficiency of cloud removal picture for AoI-1, AoI-2, and AoI-3 was 99.67%, 76.51%, and 98.34%, respectively, using the BCR model with the case of the 2013-2015 period or 33 images of acquisition in AoI. The average efficiency of these three AoI's was 91.50%. It signifies that all BCR models produce a cloud cover image with a value of less than or equal to 10%.

In many cases, cloud removal models like this help users in their frustration to get cloud-free satellite images. The assistance will be significant, especially for areas that were always covered with clouds throughout the year, such as in areas around the equator. Given the importance of spatial information of cloud coverage over an image for users ordering satellite images, it was strongly advised to develop automatic applications using machine learning at a later stage.

ACKNOWLEDGEMENTS

The authors would like to thank PT. Terramitra Citra Persada, Jakarta, Indonesia to support process equipment and research assistance. To the the Department of Geography, Faculty of Mathematics and Natural Sciences, Universitas Indonesia, we thank you for the support and facilitation in completing this research. And to Maxar Technology, we thank the quick Look of high-resolution satellite images that we have accessed through its homepage.

REFERENCES

[1] U.S. Geological Survey, *Landsat 8 Data Users Handbook*, Department of the Interior U.S. Geological Survey, vol. 8, no. June, p. 97, 2016. [Online]. Available: https://www.greenpolicy360.net/mw/images/Landsat8DataUsersHandbook.pdf
[2] S. Hastenrath, "The Intertropical Convergence Zone of the Eastern Pacific Revisited," *International Journal of Climatology*, vol. 22, no. 3, pp. 347–356, Mar. 2002, doi: 10.1002/joc.739.
[3] Ministry of Law and Human Rights of the Republic of Indonesia, "Regulation of the Geospatial Information Agency of the Republic of Indonesia Number 1 of 2020 concerning Standards for Collecting Basic Geospatial Data for Making Large-Scale Base Maps," State Information of the Republic of Indonesia Year 2020 Number 154. (In Bahasa). [Online]. Available: https://peraturan.go.id/common/dokumen/bn/2020/bn154-2020.pdf
[4] R. D. Dimyati, P. Danoedoro, Hartono, and Kustiyo, "A Minimum Cloud Cover Mosaic Image Model of the Operational Land Imager Landsat-8 multi-temporal data using Tile-based," *International Journal of Electrical and Computer Engineering (IJECE)* vol. 8, no. 1, pp. 360-371, Feb. 2018, doi: 10.11591/ijece.v8i1.pp360-371.
[5] M. C. Hansen and T. R. Loveland, "A review of large area monitoring of land cover change using Landsat data," *Remote Sensing of Environment*, vol. 122, pp. 66–74, Jul. 2012, doi: 10.1016/j.rse.2011.08.024.
[6] B. A. Margono, A. B. Usman, Budiharto, and R. A. Sugardiman, "Indonesia's forest resource monitoring," *Indonesian Journal of Geography*, vol. 48, no. 1, pp. 7–20, 2016, doi: 10.22146/ijg.12496.
[7] M. Xu, X. Jia, M. Pickering and A. J. Plaza, "Cloud Removal Based on Sparse Representation via Multitemporal Dictionary Learning," in *IEEE Transactions on Geoscience and Remote Sensing*, vol. 54, no. 5, pp. 2998-3006, May 2016, doi: 10.1109/TGRS.2015.2509860.
[8] D. S. Candra, S. Phinn, and P. Scarth, "Cloud and Cloud Shadow Masking using Multi-temporal Cloud Masking Algorithm in Tropical Environmental," *23rd International Archives of the Photogrammetry, Remote Sensing and Spatial Information Sciences*, 2016, vol. 41 no. B2, pp. 95-100, doi: 10.5194/isprs-archives-XLI-B2-95-2016.
[9] S. Das, P. Das, and B. R. Roy, "Cloud Detection and Cloud Removal of Satellite Image-A Case Study," *Conference paper: Trends in Communication, Cloud, and Big Data*, 2020, pp 53-63, doi: 10.1007/978-981-15-1624-5_6.
[10] A. Meraner, P. Ebel, X. X. Zhu, and M. Schmitt, "Cloud removal in Sentinel-2 imagery using a deep residual neural network and SAR-optical data fusion," *ISPRS Journal of Photogrammetry and Remote Sensing*, vol. 166, pp. 333-346, doi: 10.1016/j.isprsjprs.2020.05.013.
[11] T. Wang, J. Shi, H. Letu, Y. Ma, X. Li, and Y. Zheng, "Detection and Removal of Clouds and Associated Shadows in Satellite Imagery-Based on Simulated Radiance Fields," *Journal of Geophysical Research Atmospheres*, vol. 124, no. 13, pp. 7207-7225. Jun. 2019, doi: 10.1029/2018JD029960.
[12] S. H. Puteri, "The Difference of Filtering Clouds and Masking Cloud in Google Earth Engine," May 2020. [Online]. Available: https://sryhandiniputeri.medium.com/the-difference-of-filtering-clouds-and-masking-cloud-in-google-earth-engine-260744bcc600.
[13] K. Tarrio *et al.*, "Comparison of cloud detection algorithms for Sentinel-2 imagery," *Science of Remote Sensing*, Vol. 2, Dec 2020, doi: 10.1016/j.srs.2020.100010.
[14] K. Kalkan and M. D. Maktav, "A Cloud Removal Algorithm to Generate Cloud and Cloud Shadow Free Images Using Information Cloning," *Journal of the Indian Society of Remote Sensing*, vol. 46, no. 11, doi: 10.1007/s12524-018-0806-y.
[15] Y. Zi, F. Xie, and Z. Jiang, "A Cloud Detection Method for Landsat 8 Images Based on PCANet," *Remote Sensing*, vol. 10, no.6, Jun. 2018, doi:10.3390/rs10060877.
[16] Z. Li, H. Shen, Q. Cheng, W. Li, and L. Zhang, "Thick Cloud Removal in High-Resolution Satellite Images Using Stepwise Radiometric Adjustment and Residual Correction," *Remote Sensing*, vol. 11, no. 16, Jun. 2019, doi: 10.3390/rs11161925.
[17] R. D. Dimyati, P. Danoedoro, Hartono, Kustiyo, and M. Dimyati, "Digital Interpretability of Annual Tile-based Mosaic of Landsat-8 OLI for Time-series Land Cover Analysis in the Central Part of Sumatra," *Indonesian Journal of Geography*, vol 50, no. 2, 2018, doi: 10.22146/ijg.35046.
[18] Y. Guo, F. Li, P. Caccetta, D. Devereux, and M. Berman, "Cloud filtering for Landsat TM satellite images using multiple temporal mosaicing," *2016 IEEE International Geoscience and Remote Sensing Symposium (IGARSS)*, 2016, pp. 7240-7243, doi: 10.1109/IGARSS.2016.7730888.
[19] B. Chen, B. Huang, L. Chen, and B. Xu, "Spatially and Temporally Weighted Regression: A Novel Method to Produce Continuous Cloud-Free Landsat Imagery," in *IEEE Transactions on Geoscience and Remote Sensing*, vol. 55, no. 1, pp. 27-37, Jan. 2017, doi: 10.1109/TGRS.2016.2580576.
[20] Kustiyo, "Development of Annual Landsat 8 Composite Over Central Kalimantan, Indonesia Using Automatic Algorithm to Minimize Cloud," *International Journal of Remote Sensing and Earth Sciences (IJReSES)*, vol. 13, no. 1, p. 51, 2016, doi: 10.30536/j.ijreses.2016.v13.a2714.
[21] eoPortal News, "MDA closes DigitalGlobe merger, re-brands as Maxar Technologies," October 2017. [Online]. Available: https://eoportal.org/web/eoportal/news/research/-/article/mda-closes-digitalglobe-merger-re-brands-as-maxar-technologies (accessed June 26, 2021).
[22] Maxar Technology. "Area of Interest". https://discover.digitalglobe.com/ (accessed May 1, 2021).
[23] P. Maglione, C. Parente, and A. Vallario, "Using Worldview-2 Satellite Imagery To Support Geoscience Studies On Phlegraean Area," *American Journal of Geosciences*, vol. 3, no. 1, pp. 1-12, 2013, doi: 10.3844/ajgsp.2013.1.12.
[24] H. Park, N. Kim, S. Park, and J Choi, "Sharpening of Worldview-3 Satellite Images by Generating Optimal High-Spatial-Resolution Images," *Applied Science*, vol. 10, no. 20, Oct. 2020, doi: 10.3390/app10207313.
[25] GISGeography, "Global Mapper Software by Blue Marble (Review)", June 9, 2021. [Online]. Available: https://gisgeography.com/global-mapper-software-blue-marble/ (accessed June 26, 2021).
[26] H. Smith. "Deep Dive into ArcGIS Maps for Adobe with Photoshop", June, 2021. Available: https://www.esri.com/arcgis-blog/products/maps-for-adobecc/mapping/use-arcgis-map-data-in-photoshop/ (accessed June 26, 2021).
[27] H. Xu and J. Lenhardt, "Clean up your Landsst imagery: removing cloud and cloud shadow," esri, ArcGIS Blog, December 2020. [Online]. Available: https://www.esri.com/arcgis-blog/products/arcgis-pro/imagery/clean-up-your-landsat-imagery-removing-cloud-and-cloud-shadow/ (accessed on June 26, 2021).
[28] Earth Observing System, "High-resolution atellite imagery," [Online]. Available: https://eos.com/products/high-resolution-images/ (accessed on June 26, 2021).

[29] Ministry of Law and Human Rights of the Republic of Indonesia, "Presidential Regulation (Perpres) No. 9 Year 2016 on the Acceleration of One Map Policy Implementation at the Level of Map Accuracy Scale 1: 50,000", State Information of the Republic of Indonesia Year 2016 Number 28. (in Bahasa). [Online]. Available: https://peraturan.bpk.go.id/Home/Details/38518/perpres-no-9-tahun-2016 (accessed June 26, 2021).
[30] F. Adam, M. Monks, T. Esch, and M. Datcu, "Cloud Removal in High Resolution Multispectral Satellite Imagery: Comparing Three Approaches," *The 2nd International Electronic Conference on Remote Sensing (ECRS 2018)*, 2018, Vol. 2, doi: 10.3390/ecrs-2-05166.

BIOGRAPHIES OF AUTHORS

Muhammad Dimyati was born in Solo. He obtained his BSc (1982) from the Faculty of Geography, Department of Remote Sensing, Gadjah Mada University, and Master (1990) and Doctoral Degree (1997) of Agricultural Science, Lab of Regional Planning, Tropical Agriculture Division, Faculty of Agriculture, Kyoto University, Japan. Since 1983-2005, he has been working for the Ministry of Public Works, in the field of Remote Sensing, Geographic Information Systems, and Spatial Planning. He was the Deputy Assistant of Large Scale Area Development, then Deputy Assistant of Integrated Infrastructure, then Deputy Assistant of Cooperation and Partnerships, then Deputy Assistant of Formal Housing Planning of the Ministry of Housings (2005-2014). He was the Deputy of Resources for Science and Technology of the Ministry of Science and Technology (2014-2015). He was a Director General of Strengthening for Research and Development, Ministry of Research, Technology, and Higher Education (2015-2020). Currently, he is an Associate Professor in the Department of Geography, Faculty of Mathematics and Natural Sciences, Universitas Indonesia. He can be contacted at email: m.dimyati@sci.ui.ac.id, muh.dimyati@yahoo.com.

Adlyani Husna was born in West Sumatera. She obtained her Bachelor's Degree in Engineering (2019) from the Faculty of Engineering, Department of Geodetic Engineering, Gadjah Mada University. She has been working for one of the mapping consultants companies as Photogrammetry and LiDAR staff. She has completed several projects related to aerial photography mapping, lidar, and GIS analysis. She is a Researcher at PT Terramitra Citra Persada, but she is currently working on a GIS analysis project for the work of the Ministry of National Land Agency. She can be contacted at email: adlyanihusna.daulay@gmail.com.

Puji Tri Handayani was born in Bogor. West Java. She is a graduate student of Bachelor of Agriculture (2016), Faculty of Agriculture, Universitas Gadjah Mada. She is also a Researcher and Sales Engineer at PT Terramitra Citra Persada. She can be contacted at email: puji@terramitra.com; pujitrihandayani26@gmail.com

Devy Nur Annisa was born in Bandung, West Java. She obtained her Bachelor's Degree from the Geodetic Engineering Study Program at Institut Teknologi Nasional Bandung (2020). She is also actively participating in the Asian Conference of Remote Sensing in 2020 as a presenter on the topic Remote Sensing for Climate Change. Currently, she is working at PT Terramitra Citra Persada as a Sales Engineer. She can be contacted at email: devy@terramitra.com; devynurannisa@gmail.com